

1-1-1987

Hydrodynamic Fluctuations in a Fluid under Constant Shear

Alejandro Garcia

San Jose State University, alejandro.garcia@sjsu.edu

M. Malek Mansour

Universite Libre de Bruxelles

G. Lie

E. Clementi

M. Mareschal

Universite Libre de Bruxelles

Follow this and additional works at: https://scholarworks.sjsu.edu/physics_astron_pub



Part of the [Other Astrophysics and Astronomy Commons](#), and the [Other Physics Commons](#)

Recommended Citation

Alejandro Garcia, M. Malek Mansour, G. Lie, E. Clementi, and M. Mareschal. "Hydrodynamic Fluctuations in a Fluid under Constant Shear" *Physical Review A* (1987): 4348-4355. <https://doi.org/http://dx.doi.org/10.1103/PhysRevA.36.4348>

This Article is brought to you for free and open access by the Physics and Astronomy at SJSU ScholarWorks. It has been accepted for inclusion in Faculty Publications by an authorized administrator of SJSU ScholarWorks. For more information, please contact scholarworks@sjsu.edu.

Hydrodynamic fluctuations in a dilute gas under shear

A. L. Garcia,* M. Malek Mansour,[†] G. C. Lie, M. Mareschal,[†] and E. Clementi
IBM Corporation (Department 48B, Mail Stop 428), Neighborhood Road, Kingston, New York 12401
 (Received 4 May 1987)

The correlation of fluctuations of a fluid in a finite container subject to a constant strain is studied with use of both the fluctuating hydrodynamics formalism and a Boltzmann Monte Carlo particle simulation. Good quantitative agreement is demonstrated.

I. INTRODUCTION

Consider a simple fluid contained between a pair of parallel planes at $y=0$ and $y=L$ which act as infinite reservoirs; by fixing the velocities and temperatures of the reservoirs, one can impose the desired nonequilibrium constraint on the system. We take the plates to be at equal temperatures; one is fixed and the other moves with a constant velocity in the x direction. The flow is laminar and the fluid evolves towards a stationary nonequilibrium steady state at which the velocity gradient, $\varphi=du/dy$, is constant. This state is stable and the fluctuations about it are small. The nature of the fluctuations, however, is significantly different from those at thermodynamic equilibrium.¹ In particular, at equilibrium the static (equal-time) correlations of the fluctuations are short ranged, and the order of a mean free path, thus hydrodynamically they are of the form²

$$\langle \delta a(\mathbf{r}) \delta b(\mathbf{r}') \rangle = \begin{cases} A \delta(\mathbf{r}-\mathbf{r}'), & a=b \\ 0, & a \neq b \end{cases} \quad (\text{equilibrium}) \quad (1)$$

where a and b are density, velocity, or temperature. Out of equilibrium, however, some of the static correlations acquire a long-range component. This, in turn, will modify the dynamical correlation functions, for example, the dynamical structure function measured in light scattering experiments.³

These nonequilibrium modifications are now well known and have been predicted by a variety of theoretical approaches⁴⁻⁹ (for a recent review see Ref. 10). Yet, while light scattering experiments confirm the theoretical predictions in systems with a temperature gradient,¹¹ no corresponding results exist for systems with a velocity gradient. The predicted strain necessary to produce an observable effect while still maintaining laminar flow is difficult to achieve in the laboratory.⁴ Colloidal suspensions, however, are useful in the study of nonequilibrium modifications in the radial distribution function.¹²

Computer particle simulations provide an alternative "experimental" approach. By molecular-dynamics simulations, much is now known about the macroscopic properties of fluids.¹³ The existence of non-Newtonian behavior, such as shear thinning (shear viscosity decreasing with increasing shear rate) and shear dilatancy (hydrostatic pressure increasing with increasing shear rate) in simple fluids is now well established.¹⁴ While a

kinetic-theory formulation is required for a complete description of these phenomena, it is believed that mode coupling of microscopic fluctuations plays an important part,^{9,15,16} somewhat in analogy with the effective viscosity defined for turbulent flows.¹⁷

Recently, we have employed a stochastic particle simulation¹⁸ to study hydrodynamic fluctuations in a dilute gas under a constant temperature difference.^{19,20} In this paper, we extend our studies to the shear problem and compare the simulation results with two fluctuating hydrodynamics calculations.²¹ The first is an exactly soluble model which qualitatively describes well the simulation results. Next, from the full fluctuating hydrodynamics equations for a dilute gas the correlation functions are obtained numerically. In the latter calculation, the agreement with the simulation data is found to be quantitatively very good for a large system (20 000 particles, $L=50$ mean free paths) and fair for a small system (4000 particles, $L=10$ mean free paths). The calculations presented differ from previous work principally in the dominating influence of the boundary conditions in our systems, whose sizes are only tens of mean free paths.

II. COMPUTER SIMULATION FOR A DILUTE GAS

For our computer experiments we chose to employ a Monte Carlo dilute-gas simulation rather than attempting a molecular dynamics (MD) approach. Our experience shows that observing nonequilibrium fluctuations, even in simple models, requires a considerable amount of statistics.^{22,23} The dilute-gas simulation (also known as DSMC, direct simulation Monte Carlo method) have been used successfully by Bird and others in the study of rarefied-gas dynamics problems.¹⁸ The simulation was originally developed to compute flow fields in the large-Knudsen-number regime [(mean free path)/(characteristic length) >0.1]. For example, it correctly yields the density profile of a high Mach number ($M > 2$) shock wave, a problem beyond the range of validity of the Navier-Stokes equations.²⁴ Collective behavior, such as buoyancy-induced convection in the slot problem, has also been observed.^{25,26} Some shortcomings in the simulation method, recently discussed by Meiburg,²⁷ have been proven by Bird to be unimportant.²⁸ Recently, we have used DSMC simulations to study fluctuations in a

system under a constant temperature gradient.^{19,20}

The DSMC simulation algorithm is described in detail in Ref. 18, yet since the method is not as well known as molecular dynamics, we give a brief sketch here. As with MD, the state of the system is the set of particle positions and velocities, $\{\mathbf{r}_i, \mathbf{v}_i\}$ where $i=1, 2, \dots, n$. The evolution of the system is integrated in time steps Δt which are typically a small fraction of the mean collision time for a particle. Within a time step, the free flight motion and the particle interactions (collisions) are assumed to be decoupled. The free flight motion for particle i is trivially computed as $\mathbf{r}_i(t+\Delta t) = \mathbf{r}_i(t) + \mathbf{v}_i(t)\Delta t$, along with the appropriate boundary conditions. In the x and z directions we take periodic boundaries; the planes $y=0$ and $y=L$ are thermal walls at fixed temperature, T_w , and fixed velocities, $\mathbf{u}(y=0)=0$ and $\mathbf{u}(y=L)=\mathbf{u}_w$, respectively. When a particle strikes a wall its velocity is reset randomly according to a half-Maxwellian distribution with the wall's temperature and velocity.¹⁸

After all the particles have been moved, they are sorted into cells, typically a fraction of a mean free path (MFP) in length (our cells are $1 \times 0.25 \times 1$ MFP in size). A set of representative collisions for the time step are chosen in each cell. The collision process in a cell is approximated by the Kac model of the Boltzmann equation.²⁹ All particles within the cell are considered to be candidate collision partners. For hard spheres, each pair in cell α is assigned a collision probability based on their relative speed,

$$P_\alpha(i, j) = |\mathbf{v}_i - \mathbf{v}_j| / \Xi_\alpha, \quad i, j \in \alpha \quad (2)$$

where the normalization of the probability density is

$$\Xi_\alpha = \frac{1}{2} \sum_{i \in \alpha} \sum_{j \in \alpha} |\mathbf{v}_i - \mathbf{v}_j| \quad (3)$$

It would be computationally expensive to compute Ξ_α for each cell at each time step. Instead, an acceptance-rejection scheme³⁰ is used to select collision pairs given $P_\alpha(i, j)$. A pair of particles (i, j) chosen at random is taken to be the next to collide if

$$\frac{|\mathbf{v}_i - \mathbf{v}_j|}{v_{\max}} > R, \quad (4)$$

where R is a uniformly distributed random number in the interval $(0, 1)$ and v_{\max} denotes the "estimated" maximum relative speed. The acceptance-rejection method is exact if

$$v_{\max} \geq \max(|\mathbf{v}_i - \mathbf{v}_j|), \quad i, j \in \alpha \quad (5)$$

and is most efficient when the equality holds. Yet computationally it is more efficient to make an intelligent guess which overestimates v_{\max} rather than compute it at each time step.

After a pair is chosen, a random impact parameter is selected and the collision is evaluated. Note that linear momentum and energy are conserved in the evaluation of the collision. Since the sequence of collisions in a cell is modeled as a Markov process, the waiting time between collisions, τ , is exponentially distributed³¹ as

$$P_\alpha(\tau) = \mu_\alpha \exp(-\mu_\alpha \tau), \quad (6)$$

where μ_α is the collision frequency in the cell. From elementary kinetic theory, for hard spheres we have

$$\mu_\alpha = \frac{\pi d^2 N_\alpha (N_\alpha - 1)}{2V_c} \langle |\mathbf{v}_i - \mathbf{v}_j| \rangle_\alpha, \quad (7)$$

where d is the particle diameter, N_α is the particle number in the cell, and V_c is the cell volume. The average $\langle \rangle_\alpha$ is over all pairs in the cell α . Since the exact evaluation of $\langle |\mathbf{v}_i - \mathbf{v}_j| \rangle_\alpha$ is computationally expensive, one typically makes the approximation

$$\langle |\mathbf{v}_i - \mathbf{v}_j| \rangle_\alpha \approx |\mathbf{v}_i - \mathbf{v}_j|, \quad (8)$$

where i and j are the particles which were selected and *accepted* on the previous collision. One can show that on average the correct collision frequency is obtained if the number of particles per cell is large (> 20). Of course, if the number of particles per cell is not large then the evaluation of $\langle |\mathbf{v}_i - \mathbf{v}_j| \rangle_\alpha$ directly is no longer computationally expensive.³²

Simulation runs were made for two systems, one small ($1 \times 10 \times 1$ MFP, 4000 particles) and the other large ($1 \times 50 \times 1$ MFP, 20 000 particles). In each case, the velocity of the moving wall was $(8k_B T_w / m)^{1/2}$ (approximately twice the sound speed) where k_B is the Boltzmann constant and m is the particle mass. The lengths and velocities in the simulation are normalized by the mean free path and the most probable molecular speed at equilibrium, respectively; the particle mass is taken as unity. For the purpose of measurement, each system was divided into a chain of 20 cells; statistics were accumulated on the state of each cell.

The program was run in parallel on two Floating Point Systems FPS-264 array processors in the 1CAP2 system at IBM Kingston. The lengths of the runs were on the order of 10^9 collisions, typically 48 hours of central-processing-unit time. In Figs. 1 and 2 we graph the measured velocity and temperature profiles for the

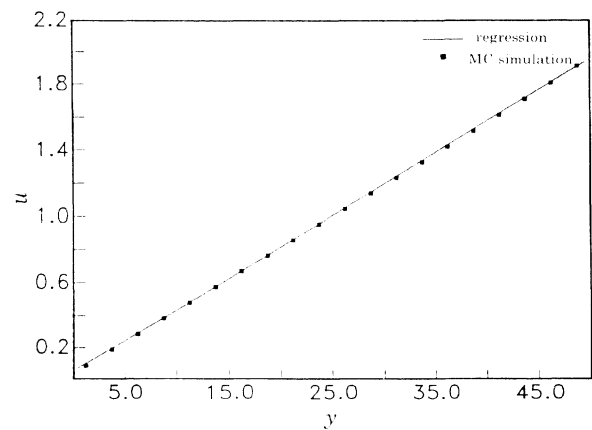


FIG. 1. Measured x -velocity profile for the large system. Parameters in the simulation were $L=50$ mean free paths, 20 000 particles, $T_w=1$, $u_w=(8RT_w)^{1/2}$, $L_x=L_z=1$ MFP, $\eta_0 = \frac{5}{16} \rho_0 (\pi T_0)^{1/2}$, $m=1$, $R = \frac{1}{2}$. The solid line is the macroscopic steady state [Eq. (43)].

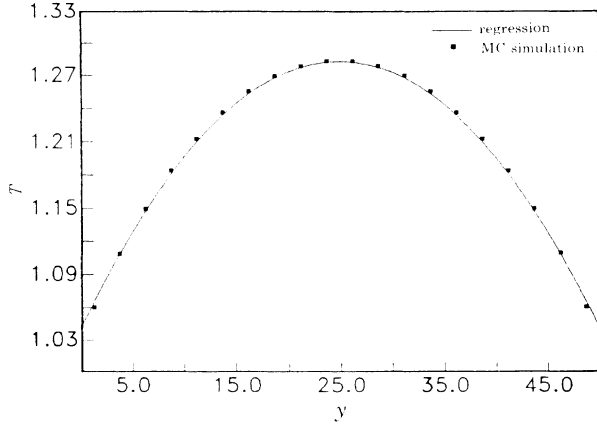


FIG. 2. Measured temperature profile in the large system; see Fig. 1 for the simulation parameters. The solid line is the macroscopic steady state [Eq. (44)].

large system. Note that even though the Knudsen number is relatively large and the strain severe the data are still extremely well described by the macroscopic hydrodynamic equations with the transport coefficients taken as constant (solid line). The error bars for the data points are about a tenth the size of the symbols marking the points. From these profiles (excluding the cells next to the walls) the Prandtl number may be computed (see also Ref. 33). For the large system we find $\bar{P}=0.6677$ and $\bar{P}=0.6805$ for the small system; the Prandtl number for a dilute gas is $\frac{2}{3}$.²¹ The deviation for the large system does not exceed 0.2% while for the small system it is close to 3%; this deviation in the small system decreases to 1% if the velocity gradient is reduced to that of the large system. The relatively larger error for the small system is probably due to the relatively large slip boundary layer at each wall. Unfortunately, some interesting predictions concerning the long-ranged extent of the slipping length were untestable within the given simulation parameters.³⁴

In Figs. 3 and 4 we present the measured static correlation function of the x -velocity fluctuations in the large and small systems, respectively. Figure 5 depicts the static correlation function of the density fluctuations measured in the large system. Note that in each case only the nonequilibrium part is displayed; the large local equilibrium delta function component,

$$\begin{aligned} \langle \delta\rho_i \delta\rho_j \rangle &= (\rho_i / V_c) \delta_{i,j} \quad (\text{equilibrium}) \\ \langle \delta u_i \delta u_j \rangle &= [k_B T_i / (\rho_i V_c)] \delta_{i,j} \quad (\text{equilibrium}), \end{aligned} \quad (9)$$

has been removed. Note that the velocity correlations in the two systems are similar in nature and are of long-range extent. These figures will be discussed further in the following sections.

III. FLUCTUATING HYDRODYNAMICS WITH A SIMPLE MODEL

In this section we show that the above results for the velocity correlations can be reproduced, at least qualita-

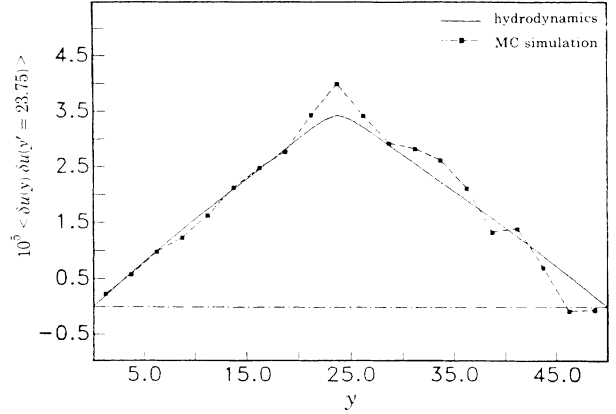


FIG. 3. Measured static correlation function for the x -velocity fluctuations, $\langle \delta u(y) \delta u(y' = \frac{10}{2l}) \rangle$, in the large system. See Fig. 1 for the simulation parameters. The solid line represents the numerical solution of the fluctuating-hydrodynamics equations for a dilute gas (see Sec. IV). The local equilibrium contribution has been removed [see Eq. (9)].

tively, by a straightforward fluctuating-hydrodynamics²¹ calculation for a model fluid. Consider a simple fluid with the following characteristics:^{6,7} the thermal expansivity vanishes, $|\partial P / \partial T|_{\rho} = 0$, the transport coefficients are constant, i.e., independent of density and temperature, and the state of the walls is statistically independent of the state of the system. By the first assumption, the momentum equation is decoupled from the energy equation.^{6,7} The last assumption implies a simple form for the boundary conditions which is precisely the one realized in our computer experiments.^{20,35} While these assumptions considerably simplify the analysis, the main physical aspects are preserved.¹⁰

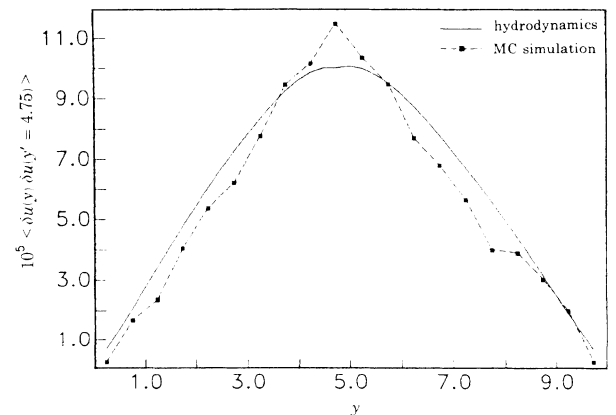


FIG. 4. Measure static correlation function for the x -velocity fluctuations, $\langle \delta u(y) \delta u(y' = \frac{10}{2l}) \rangle$, in the small system. Parameters in the simulation were $L=10$ mean free paths, 4000 particles, $T_w=1$, $u_w=(8RT_w)^{1/2}$, $L_x=L_z=1$ MFP, $\eta_0 = \frac{5}{16} \rho_0 (\pi T_0)^{1/2}$, $m=1$, $R = \frac{1}{2}$. The solid line represents the numerical solution of the fluctuating-hydrodynamics equations for a dilute gas (see Sec. IV). The local equilibrium contribution has been removed [see Eq. (9)].

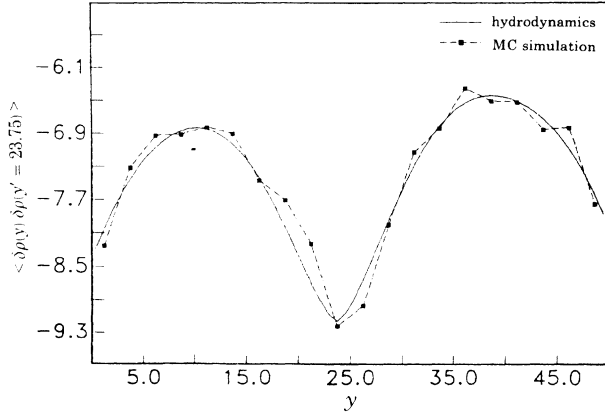


FIG. 5. Measure static correlation function for the density fluctuations, $\langle \delta\rho(y)\delta\rho(y'=\frac{10}{21}) \rangle$, in the large system. See Fig. 1 for the simulation parameters. The solid line represents the numerical solution of the fluctuating-hydrodynamics equations for a dilute gas (see Sec. IV). The local equilibrium contribution has been removed [see Eq. (9)].

It is now easy to check that the steady-state density, ρ_0 , is constant and the velocity profile is

$$\mathbf{u}_0(\mathbf{r}) = \varphi y \mathbf{I}_x, \quad (10)$$

where \mathbf{I}_x is the unit vector in the x direction, φ is the (constant) velocity gradient, and the subscript 0 denotes macroscopic quantities. Due to viscous heating, the fluid develops a parabolic temperature profile whose amplitude is proportional to the square of the imposed strain. If this strain is not too large, the temperature variation is very small (see Fig. 2) and for simplicity, we shall take the temperature as constant.

Since the boundaries in the x and z direction are periodic, we restrict ourselves to reduced variables defined by

$$\delta h(y) = \frac{1}{S} \int_0^{L_x} dx \int_0^{L_z} dz \delta h(x, y, z), \quad (11)$$

where h is any hydrodynamic variable and $S \equiv L_x L_z$ is the surface area of the walls. Note that these reduced variables are in fact the zero-wave-number values of the “parallel” Fourier components of the hydrodynamic variables. In the simulation, the system is similarly sliced into cells and statistics are collected on the states of these cells.

The linearized fluctuating-hydrodynamic equations in the reduced variables are^{20,35}

$$\frac{\partial}{\partial t} \delta\rho = -\rho_0 \frac{\partial}{\partial y} \delta v, \quad (12)$$

$$\frac{\partial}{\partial t} \delta u = -\varphi \delta v + \frac{\eta}{\rho_0} \frac{\partial^2}{\partial y^2} \delta u + \frac{1}{\rho_0} \frac{\partial}{\partial y} \sigma_{xy}(y, t), \quad (13)$$

$$\begin{aligned} \frac{\partial}{\partial t} \delta v = & -\alpha \frac{\partial}{\partial y} \delta\rho + \frac{1}{\rho_0} \left(\frac{4}{3}\eta + \zeta \right) \frac{\partial^2}{\partial y^2} \delta v \\ & + \frac{1}{\rho_0} \frac{\partial}{\partial y} \sigma_{yy}(y, t), \end{aligned} \quad (14)$$

$$\frac{\partial}{\partial t} \delta w = \frac{\eta}{\rho_0} \frac{\partial^2}{\partial y^2} \delta w + \frac{1}{\rho_0} \frac{\partial}{\partial y} \sigma_{zy}(y, t), \quad (15)$$

where $\delta\rho$, δu , δv , and δw are the density fluctuations and the x , y , and z components of the velocity fluctuations, respectively. The shear and bulk viscosities are η and ζ , respectively, and $\alpha = (1/\rho_0) | \partial P_0 / \partial \rho_0 |_T$. The stochastic components of the reduced pressure tensor, σ_{ij} , are white-noise processes with zero mean and variances,²¹

$$\begin{aligned} \langle \sigma_{ij}(y, t) \sigma_{kl}(y', t') \rangle \\ = \frac{2k_B T_0}{S} \delta(y - y') \delta(t - t') \\ \times [\eta (\delta_{ik} \delta_{jl} + \delta_{il} \delta_{jk}) + (\zeta - \eta/3) \delta_{ij} \delta_{kl}]. \end{aligned} \quad (16)$$

The boundary conditions for δv follow from the conservation of total particle number and the continuity equation

$$\rho_0 \delta v(y) |_{\text{boundaries}} = 0, \quad (17)$$

i.e., the boundary acts as a perfectly rigid wall. The boundary conditions for δu and δw are as those of a no-slip wall,

$$\delta u(y=0) = \delta u(y=L) = \delta w(y=0) = \delta w(y=L) = 0. \quad (18)$$

These relations are a consequence of our assumption that the state of the walls is statistically independent with respect to the state of the system. No boundary condition for $\delta\rho$ is required as its evolution is entirely specified by the initial conditions for $\delta\rho$ plus the boundary and initial conditions for δu , δv , and δw . From a physical point of view, this reflects the fact that the state of the wall can only constrain the temperature and velocity of the fluid at the wall whereas the behavior of the density close to the wall is entirely determined by the internal dynamics of the system. (The full mathematical aspects of this problem are discussed in Ref. 36.)

With the above boundary conditions, it is easy to show that the reduced fluctuations can be expanded in the following sine and cosine series:

$$\delta\rho(y, t) = \sum_{k=0}^{\infty} \delta\rho_k(t) \cos(k\pi y/L), \quad (19a)$$

$$\begin{bmatrix} \delta u(y, t) \\ \delta v(y, t) \\ \delta w(y, t) \end{bmatrix} = \sum_{k=0}^{\infty} \begin{bmatrix} \delta u_k(t) \\ \delta v_k(t) \\ \delta w_k(t) \end{bmatrix} \sin \left[\frac{k\pi y}{L} \right], \quad (19b)$$

with the well-known inverse formula

$$\delta\rho_k(t) = \frac{2}{L} \int_0^L dy \delta\rho(y, t) \cos(k\pi y/L), \quad \delta\rho_0(t) = 0 \quad (19c)$$

$$\begin{bmatrix} \delta u_k(t) \\ \delta v_k(t) \\ \delta w_k(t) \end{bmatrix} = \frac{2}{L} \int_0^L dy \begin{bmatrix} \delta u(y, t) \\ \delta v(y, t) \\ \delta w(y, t) \end{bmatrix} \sin \left[\frac{k\pi y}{L} \right]. \quad (19d)$$

In this paper we restrict ourselves to the study of the

statistical properties of a system in the stationary regime (i.e., we are not considering the transient regimes where one studies the evolution from a given initial condition). In this regime, a common approach is to use the Fourier transform in time,

$$\delta h(t) = \int_{-\infty}^{\infty} d\omega \delta h(\omega) e^{-i\omega t}, \quad (20a)$$

$$\delta h(\omega) = (1/2\pi) \int_{-\infty}^{\infty} dt \delta h(t) e^{i\omega t}, \quad (20b)$$

where h is any hydrodynamic variable.

Using now the transforms (19) and (20), we immediately obtain the correlation functions for the variables $\delta\rho$, δv , and δw ,

$$\begin{aligned} \langle \delta\rho_k(\omega) \delta\rho_{k'}(\omega') \rangle &= \frac{4k_B \rho_0 T_0 \Gamma}{\pi V} \frac{(k^4 \pi^4 / L^4) \delta(\omega + \omega') \delta_{kk'}}{[\omega^2 - (ck\pi/L)^2]^2 + 4\omega^2 \Gamma^2 k^4 \pi^4 / L^4}, \\ & \quad (21) \end{aligned}$$

$$\begin{aligned} \langle \delta v_k(\omega) \delta v_{k'}(\omega') \rangle &= \frac{4k_B T_0 \Gamma}{\rho_0 \pi V} \frac{(\omega^2 k^2 \pi^2 / L^2) \delta(\omega + \omega') \delta_{kk'}}{[\omega^2 - (ck\pi/L)^2]^2 + 4\omega^2 \Gamma^2 k^4 \pi^4 / L^4}, \\ & \quad (22) \end{aligned}$$

$$\langle \delta w_k(\omega) \delta w_{k'}(\omega') \rangle = \frac{2k_B T_0 \eta}{\pi V \rho_0^2} \frac{\delta(\omega + \omega') \delta_{kk'} k^2 \pi^2 / L^2}{(\eta/\rho_0)^2 k^4 \pi^4 / L^4 + \omega^2}, \quad (23)$$

$$\langle \delta\rho_k(\omega) \delta v_{k'}(\omega') \rangle = (-i\rho_0 k \pi / \omega L) \langle \delta v_k(\omega) \delta v_{k'}(\omega') \rangle, \quad (24)$$

$$\langle \delta\rho_k(\omega) \delta w_{k'}(\omega') \rangle = \langle \delta v_k(\omega) \delta w_{k'}(\omega') \rangle = 0, \quad (25)$$

where V is the volume of the system ($V = SL$), Γ is the sound damping coefficient, and c is the sound speed,

$$\Gamma = (\frac{4}{3}\eta + \zeta) / 2\rho_0, \quad (26)$$

$$c = \sqrt{\alpha\rho_0}. \quad (27)$$

In this paper we shall only consider the static correlation functions (for their dynamical behavior, see Ref. 36). For the density $\delta\rho$ and parallel velocities, δv and δw , one easily finds

$$\begin{aligned} \langle \delta v(y) \delta v(y') \rangle &= \langle \delta w(y) \delta w(y') \rangle \\ &= [k_B T_0 / (\rho_0 S)] \delta(y - y'), \end{aligned} \quad (28)$$

$$\langle \delta v(y) \delta w(y') \rangle = 0, \quad (29)$$

$$\langle \delta\rho(y) \delta\rho(y') \rangle = [k_B T_0 / (\alpha S)] [\delta(y - y') - 1/L], \quad (30)$$

which are clearly the results we expect from equilibrium statistical mechanics.² The term $-1/L$ in Eq. (30) en-

ures the conservation of the total mass. Because of this term, the static density autocorrelation function is strictly negative and its integral compensates for the local equilibrium (δ -function) contribution.

Let us now consider the reduced x component of the velocity fluctuation δu , which is the only variable affected by the velocity gradient φ . Equation (13) may be written as

$$\partial_t \delta u = \frac{\eta}{\rho_0} \frac{\partial^2}{\partial y^2} \delta u + F(y, t), \quad (31)$$

where $F(y, t)$ can be taken as an effective noise term

$$\langle F(y, t) \rangle = 0, \quad (32a)$$

$$\begin{aligned} \langle F(y, t) F(y', t') \rangle &= \frac{2k_B T_0 \eta}{\rho_0^2 S} \delta(t - t') \frac{\partial^2}{\partial y \partial y'} \delta(y - y') \\ & \quad + \varphi^2 \langle \delta v(y, t) \delta v(y', t') \rangle. \end{aligned} \quad (32b)$$

This is a *non-Markovian* equation for $\delta u(y, t)$ since $\langle \delta v(y, t) \delta v(y', t') \rangle$ is *not* δ -correlated in time.³⁶ Again, using the transforms (19) and (20), we obtain

$$\delta u_k(\omega) = \frac{-\beta_k(\omega)}{k^2 \pi^2 / \rho_0 L^2 - i\omega} - \frac{(k\pi / \rho_0 L) \psi_k(\omega)}{k^2 \pi^2 / \rho_0 L^2 - i\omega}, \quad (33)$$

where $\psi_k(\omega)$ is the Fourier transform of σ_{xy} ,

$$\langle \psi_k(\omega) \psi_{k'}(\omega') \rangle = [2k_B T_0 \eta / (\pi V)] \delta_{kk'} \delta(\omega + \omega') \quad (34)$$

and

$$\langle \beta_k(\omega) \beta_{k'}(\omega') \rangle = \varphi^2 \langle v_k(\omega) v_{k'}(\omega') \rangle. \quad (35)$$

Moreover, because of the absence of correlation between Langevin source terms, we have

$$\langle \beta_k(\omega) \psi_{k'}(\omega') \rangle = \langle \delta v_k(\omega) \psi_{k'}(\omega') \rangle = 0. \quad (36)$$

Using the relations (34)–(36) it is easy to check that

$$\begin{aligned} \langle \delta u_k(\omega) \delta u_{k'}(\omega') \rangle &= \frac{1}{(\eta/\rho_0)^2 k^4 \pi^4 / L^4 + \omega^2} \\ & \quad \times \left[\varphi^2 \langle \delta v_k(\omega) \delta v_{k'}(\omega') \rangle \right. \\ & \quad \left. + \frac{2k_B T_0 \eta}{\pi V \rho_0^2} \delta_{k,k'} \delta(\omega + \omega') \frac{k^2 \pi^2}{L^2} \right]. \end{aligned} \quad (37)$$

Integrating $\langle \delta u_k(\omega) \delta u_{k'}(\omega') \rangle$ over ω and ω' to obtain the equal-time spatial correlation and transforming back to real space, one finds, after some algebraic manipulations,

$$\langle \delta u(y) \delta u(y') \rangle - \frac{k_B T_0}{\rho_0 S} \delta(y - y') = \frac{\varphi^2}{c^2} \frac{k_B T_0}{\rho_0 S} \left[y' \left[1 - \frac{y}{L} \right] - \frac{\lambda}{2} \frac{\cosh[(y - y' - L)/\lambda] - \cosh[(y + y' - L)/\lambda]}{\sinh(L/\lambda)} \right], \quad (38a)$$

with $y > y'$ (for $y < y'$, exchange y and y') and

$$\lambda = [\eta(\xi + \frac{7}{3}\eta)]^{1/2}/(\rho_0 c). \quad (38b)$$

In Fig. 6 we depict the rhs of Eq. (38a) for various values of λ and note the good qualitative agreement with the simulation results (compare with Figs. 3 and 4). Even quantitative agreement is reasonable; predicted peak values are $\approx 3 \times 10^{-5}$ (large system) and $\approx 1 \times 10^{-4}$ (small system). Note, however, that our simple model is not adequate in describing $\langle \delta\rho \delta\rho' \rangle$ since it predicts a constant value, Eq. (30), and not the observed sinusoidal form (see Fig. 5).

The parameter λ , which has the units of length, can be associated with an acoustic absorption scale. If $\lambda \ll L$, the second term in the brackets in Eq. (38a) is negligible and the nonequilibrium part of $\langle \delta u \delta u' \rangle$ reduces to a piecewise linear function whose amplitude is proportional to the square of the amplitude of the constraint. This is reminiscent of the results of Ref. 37 for the temperature autocorrelation function in a high Prandtl number liquid (see also Refs. 19, 20, and 35) and of the results of Ref. 38 for the density autocorrelation function in a lattice gas. For $\lambda \gg L$, the entire nonequilibrium effect disappears.

IV. FLUCTUATING HYDRODYNAMICS FOR A DILUTE GAS

In this section we obtain the correlation equations for a dilute gas from the nonequilibrium fluctuating-

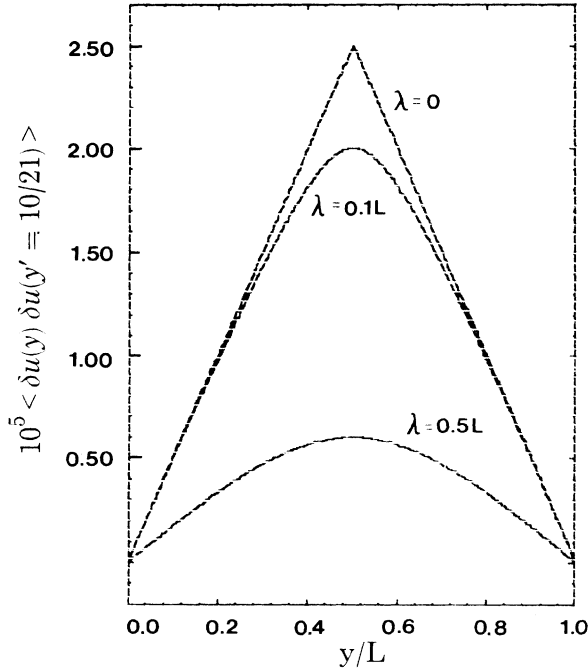


FIG. 6. Static correlation function for the x -velocity fluctuations, $\langle \delta u(y) \delta u(y' = \frac{10}{21}) \rangle$, for the model presented in Sec. III [see Eq. (38)]. The three curves displayed are for the values $\lambda = 0$ in the upper most curve, $\lambda = 0.1L$ in the center curve, and $\lambda = 0.5L$ in the lower curve. In each case the other parameters are as for the large system (see Fig. 1). The local equilibrium contribution has been removed [see Eq. (9)].

hydrodynamic equations. The notation is as in Sec. III and the discussion follows that of Refs. (20) and (35). Again, we only consider reduced variables as defined by Eq. (11). The fluctuating-hydrodynamic equations for the reduced density, velocity and temperature fluctuations are

$$\frac{\partial}{\partial t} \delta\rho = -\frac{\partial}{\partial y} \rho_0 \delta v, \quad (39)$$

$$\rho_0 \frac{\partial}{\partial t} \delta \mathbf{u} = -\rho_0 \varphi \delta v \mathbf{I}_x - R \frac{\partial}{\partial y} (T_0 \delta\rho + \rho_0 \delta T) \mathbf{I}_y + \frac{1}{3} \eta \frac{\partial^2}{\partial y^2} \delta v \mathbf{I}_y + \eta \frac{\partial^2}{\partial y^2} \delta \mathbf{u} - \frac{\partial}{\partial y} \sigma_{iy} \mathbf{I}_i, \quad (40)$$

$$\frac{3}{2} \rho_0 R \frac{\partial}{\partial t} \delta T = -\frac{3}{2} R \rho_0 \delta v \frac{\partial}{\partial y} T_0 - R \rho_0 T_0 \frac{\partial}{\partial y} \delta v + 2\eta \varphi \frac{\partial}{\partial y} \delta u - \varphi \sigma_{xy} + \kappa \frac{\partial^2}{\partial y^2} \delta T - \frac{\partial}{\partial y} g_y, \quad (41)$$

where κ is the thermal conductivity and $R = k_B/m$. The random components of the pressure and heat flux are white-noise processes with covariances given by Eq. (16) and

$$\langle g_y(y, t) g_y(y', t') \rangle = \frac{2k_B \kappa T_0(y)^2}{S} \delta(y - y') \delta(t - t'). \quad (42)$$

For a hard-sphere gas, the transport coefficients are functions of temperature as $\eta, \kappa \propto \sqrt{T}$; since the temperature variation is small we take the transport coefficients as constants. The bulk viscosity of a dilute gas is zero. The macroscopic variables are

$$\mathbf{u}_0(y) = \varphi y \mathbf{I}_x, \quad (43)$$

$$T_0(y) = \frac{\eta \varphi^2}{2\kappa} y(L - y) + T_w, \quad (44)$$

$$\rho_{0(y)} = \frac{P_0}{RT_0(y)}, \quad (45)$$

where the hydrostatic pressure P_0 is a constant. Our boundary conditions for $\delta \mathbf{u}$ are still given by Eqs. (17) and (18); by similar arguments, our boundary condition for the temperature is

$$\delta T(y=0, t) = \delta T(y=L, t) = 0. \quad (46)$$

Again, there is no boundary condition for $\delta\rho$.

Because the coefficients and the noise are both space dependent, it is not possible to proceed in the same manner as in Sec. III. Yet, using some basic identities of stochastic processes, it is possible to write a set of coupled equations for the static correlations $\langle \delta a(y) \delta b(y') \rangle$.^{20, 35, 39} For example, for the $\langle \delta u(y) \delta u(y') \rangle$ static correlations, we have

$$\begin{aligned} \rho_0 \varphi_0 \frac{\partial}{\partial t} \langle \delta u \delta u' \rangle &= 0 = -\varphi \rho_0 \varphi_0' (\langle \delta v \delta u' \rangle + \langle \delta u \delta v' \rangle) \\ &+ \eta \left[\rho_0' \frac{\partial^2}{\partial y^2} + \rho_0 \frac{\partial^2}{\partial y'^2} \right] \langle \delta u \delta u' \rangle \\ &+ \frac{\partial^2}{\partial y \partial y'} \langle \sigma_{xy} \sigma_{xy}' \rangle. \end{aligned} \quad (47)$$

Naturally, we must solve the full set of coupled equations, a task we have only succeeded to do numerically. In Figs. 3–5, the solid curves are the numerical solutions we obtain using the parameters from our particle simulations (see Sec. II). Agreement is very good for the large system while only fair for the small system. We believe this is due to the effect of the slip boundary layer; as the wall velocity is the same in the two systems the strain in the small system is five times greater. Recall that the measured Prandtl number in the small system was also different from the value predicted by kinetic theory [the theoretical values were used in the numerical solution of Eqs. (39)–(41)]. In Fig. 5 we see that the sinusoidal form for $\langle \delta\rho \delta\rho' \rangle$ is recovered, in contrast with the result for the simple model in Sec. III.

V. CONCLUSIONS

In this paper we have studied a dilute gas under shear by means of a Boltzmann Monte Carlo simulation originally developed by Bird.¹⁸ In our previous work the same technique was applied to the study of a system held at a constant temperature difference.²⁰ In both cases, the results were compared with those obtained by direct application of the Landau-Lifshitz fluctuating-hydrodynamics formalism and nice quantitative agreement was demonstrated for the static correlation functions. We also have some preliminary results which indicate that this success extends to the dynamic correlation functions, such as the dynamical scattering function.⁴⁰ These results are sufficiently encouraging to warrant an investigation of the onset of instabilities, such as the Rayleigh-Bénard problem,⁴¹ by this approach.

The direct conclusion is obviously the applicability of the fluctuating-hydrodynamics formalism down to a few mean free paths even in systems under severe nonequilibrium constraints. Yet, another interpretation is possible. Fluctuating hydrodynamics has a well established theoretical foundation for near-equilibrium systems. It can be derived from kinetic theory and its applicability appears to be only limited by the validity of the local equilibrium hypothesis (see also Ref. 42). Light scattering measurements in nonequilibrium systems add further experimental evidence to this assertion.¹¹

On the contrary, there exists no similar theoretical support for the stochastic Boltzmann-equation simulation; its validation lies in its success in reproducing laboratory results such as shock-wave profiles. While the Kac model for the collision process is well established, the simple treatment of transport processes adopted in the simulation (the transport and collision processes are decoupled during a timestep), has not received any seri-

ous theoretical investigation. Thus, the agreement between simulation data and fluctuating-hydrodynamics calculations in *near-equilibrium* systems may be seen as demonstrating the applicability of the Boltzmann Monte Carlo approach for the study of fluctuations. The results presented in this paper further suggest to us that both fluctuating hydrodynamics and the DSMC approach are valid in *far-from-equilibrium* systems.

This assertion, of course, needs to be checked more extensively, yet if it is true then a great advance towards computer experiments of nonequilibrium systems is achieved. The classical molecular-dynamics experiments were originally developed to study the statistical properties of equilibrium systems. Their extension to nonequilibrium systems was oriented, mainly, to the study of the macroscopic behavior of fluids and many interesting properties were discovered (see the Introduction and Ref. 12). Yet even with modern supercomputers, it is computationally prohibitively expensive to study nonequilibrium modifications to the correlation of fluctuations via molecular dynamics.

The stochastic approach in particle simulations, such as the one presented here, gives one an interesting alternative. First and most importantly, our evidence indicates that it correctly reproduces microscopic fluctuations in far from equilibrium systems as compared with the Landau-Lifshitz formalism. This is a non-negligible advantage over other computational models, such as the one based on cellular automata, where only the macroscopic properties are well established.⁴³ Second, the method appears to be applicable to large-Knudsen-number systems. While this assertion is well tested for macroscopic properties, it remains to be checked that the method correctly describes fluctuations for all values of Knudsen number. The main limitation in the stochastic approach is that, currently, it has only been formulated for a dilute gas. Whether or not a direct simulation Monte Carlo method can be set up for a liquid remains an open question. However, a generalization of the technique for a moderately dense gas based on the Enskog equation seems possible;⁴⁴ work in this direction is in progress.

ACKNOWLEDGMENTS

The authors wish to thank Professor G. Nicolis, Professor J. W. Turner, Dr. D. Kondepudi, and Dr. F. Baras for stimulating discussions. As always, we have greatly profited from the challenging questions posed and the insightful comments given by Professor Ilya Prigogine.

*Present address: Department of Mathematics, University of California, Los Angeles, CA 90024.

†Permanent address: Faculté des Sciences, Université Libre de Bruxelles (Code Postal 231), Campus Plaine, Boulevard du

Triomphe, B-1050 Bruxelles, Belgium.

¹G. Nicolis and I. Prigogine, *Self-Organisation in Nonequilibrium Systems* (Wiley, New York, 1977).

²L. D. Landau and E. M. Lifschitz, *Statistical Physics* (Per-

- gamon, Oxford, 1980), Part I.
- ³B. J. Berne and R. Pecora, *Dynamic Light Scattering* (Wiley, New York, 1976); J. P. Boon and S. Yip, *Molecular Hydrodynamics* (McGraw-Hill, New York, 1980).
- ⁴J. Machta, I. Procaccia, and I. Oppenheim, Phys. Rev. Lett. **42**, 1368 (1979); J. Machta, I. Oppenheim, and I. Procaccia, Phys. Rev. A **22**, 2809 (1980).
- ⁵T. R. Kirkpatrick, E. G. D. Cohen, and J. R. Dorfman, Phys. Rev. Lett. **42**, 862 (1979); Phys. Rev. Lett. **44**, 472 (1980); Phys. Rev. A **26**, 950 (1982); Phys. Rev. A **26**, 972 (1982).
- ⁶I. Procaccia, D. Ronis, and I. Oppenheim, Phys. Rev. Lett. **42**, 287 (1979); D. Ronis, I. Procaccia, and I. Oppenheim, Phys. Rev. A **19**, 1324 (1979); D. Ronis and S. Putterman, *ibid.* **22**, 773 (1980); D. Ronis and I. Procaccia, **26**, 1812 (1982).
- ⁷A. M. Tremblay, E. D. Siggia, and M. R. Arai, Phys. Lett. **76A**, 57 (1980).
- ⁸G. van der Zwan, D. Bedaux, and P. Mazur, Physica **107A**, 491 (1981).
- ⁹J. Lutsko and J. W. Dufty, Phys. Rev. A **32**, 1229 (1985).
- ¹⁰A. M. Tremblay, in *Recent Developments in Nonequilibrium Thermodynamics*, edited by J. Casas-Vasquez, D. Jou, and G. Lebon (Springer-Verlag, Berlin, 1984).
- ¹¹D. Beysens, Y. Garrabos, and G. Zalczer, Phys. Rev. Lett. **45**, 403 (1980); D. Beysens, Physica **118A**, 250 (1983); R. Penney, H. Kiefte, and J. M. Clouter, Bull. Can. Assoc. Phys. **39**, BB8 (1983); G. H. Wegdam, N. M. Keulen, and J. C. F. Michielsen, Phys. Rev. Lett. **55**, 630 (1985); see Ref. 10 for a review of the theoretical aspects of the temperature-gradient problem.
- ¹²N. A. Clark and B. J. Ackerson, Phys. Rev. Lett. **44**, 1005 (1980); B. J. Ackerson and N. A. Clark, Physica **83A**, 221 (1983); H. J. M. Hanley, J. C. Rainwater, N. A. Clark, and B. J. Ackerson, J. Chem. Phys. **79**, 4448 (1983).
- ¹³Proceedings of the Conference on Nonlinear Fluid Behavior, University of Colorado, Boulder, 1982 [Physica **118A**, (1983)]; Special issue on nonequilibrium fluids, Phys. Today **37**(1), (1984).
- ¹⁴D. J. Evans, Phys. Lett. **74A**, 229 (1979); S. Hess, H. J. M. Hanley, and N. Herdegen, *ibid.* **105A**, 238 (1984); W. G. Hoover, Physica **118A**, 111 (1983); D. J. Evans, *ibid.* **118A**, 51 (1983); C. Trozzi and G. Ciccotti, Phys. Rev. A **29**, 916 (1984).
- ¹⁵K. Kawasaki and J. Gunton, Phys. Rev. A **8**, 2048 (1973); T. Yamada and K. Kawasaki, Prog. Theor. Phys. **53**, 111 (1975).
- ¹⁶M. H. Ernst, B. Cichocki, J. R. Dorfman, J. Sharma, and H. van Beijeren, J. Stat. Phys. **18**, 237 (1978); T. R. Kirkpatrick, Phys. Rev. Lett. **53**, 1735 (1984); T. R. Kirkpatrick, J. Non-Crystall. Solids **75**, 437 (1985); J. Lutsko and J. W. Dufty, Phys. Rev. A **32**, 3040 (1985).
- ¹⁷V. Yakhot and S. A. Orszag, Phys. Rev. Lett. **57**, 1722 (1986); D. C. Leslie, *Developments in the Theory of Turbulence* (Oxford Science, Oxford, 1973).
- ¹⁸G. A. Bird, *Molecular Gas Dynamics* (Clarendon, Oxford, 1976).
- ¹⁹A. Garcia, Phys. Rev. A **34**, 1454 (1986).
- ²⁰M. Malek Mansour, A. Garcia, G. Lie, and E. Clementi, Phys. Rev. Lett. **58**, 874 (1987).
- ²¹L. D. Landau and E. M. Lifschitz, *Fluid Mechanics* (Pergamon, Oxford, 1959).
- ²²A. Garcia, Ph.D. thesis, The University of Texas at Austin, 1984.
- ²³M. Mareschal and E. Kestemont, Phys. Rev. A **30**, 1158 (1984).
- ²⁴R. E. Meyer, *Introduction to Mathematical Fluid Mechanics* (Dover, New York, 1971); G. A. Bird, Phys. Fluids **13**, 1172 (1970).
- ²⁵G. K. Batchelor, Q. Appl. Math. **12**, 209 (1954); D. R. Chenoweth and S. Paolucci, Phys. Fluids **28**, 2365 (1985).
- ²⁶A. Garcia and V. Mityakov (unpublished).
- ²⁷E. Meiburg, Phys. Fluids **29**, 3107 (1986).
- ²⁸G. A. Bird, Phys. Fluids **30**, 364 (1987).
- ²⁹M. Kac, in *Probability Theory and Related Topics in Physical Science* (Wiley-Interscience, New York, 1959); J. Logan and M. Kac, Phys. Rev. A **13**, 458 (1976); M. Malek Mansour, L. Brenig, and W. Horsthemke, Physica **88A**, 407 (1977); A. Onuki, J. Stat. Phys. **18**, 475 (1978); L. Brenig and C. van den Broeck, Phys. Rev. A **21**, 1039 (1980).
- ³⁰*Handbook of Mathematical Functions*, 9th ed., edited by M. Abramowitz and I. Stegun (Dover, New York, 1972).
- ³¹L. Arnold, *Stochastic Differential Equations: Theory and Applications* (Wiley, New York, 1973).
- ³²O. M. Belotserkovsky, A. I. Erofeev, and V. E. Yanitsky, in *Numerical Methods in Fluid Dynamics*, edited by N. N. Yanenko and Y. I. Shokin (Mir, Moscow, 1984).
- ³³L. Hannon, G. C. Lie, and E. Clementi, Phys. Lett. **119**, 174 (1986).
- ³⁴P. G. Wolynes, Phys. Rev. A **13**, 1235 (1976); J. C. Nieuwoudt, T. R. Kirkpatrick, and J. R. Dorfman, J. Stat. Phys. **34**, 203 (1984).
- ³⁵A. Garcia, M. Malek Mansour, G. Lie, and E. Clementi, J. Stat. Phys. **47**, 209 (1987).
- ³⁶M. Malek Mansour, J. W. Turner, and A. Garcia, J. Stat. Phys. (to be published).
- ³⁷G. Nicolis and M. Malek Mansour, Phys. Rev. A **29**, 2845 (1984).
- ³⁸H. Spohn, J. Phys. A **16**, 4275 (1983).
- ³⁹J. W. Dufty, J. J. Brey, and M. C. Marchetti, Phys. Rev. A **33**, 4307 (1986).
- ⁴⁰G. C. Lie, A. Garcia, M. Malek Mansour, and E. Clementi (unpublished).
- ⁴¹V. M. Zaitsev and M. I. Shliomis, Zh. Eksp. Teor. Fiz. **59**, 1583 (1970) [Sov. Phys.—JETP **32**, 866 (1971)]; H. N. W. Lekkerkerker and J. P. Boon, Phys. Rev. A **10**, 1355 (1974); T. R. Kirkpatrick and E. G. D. Cohen, J. Stat. Phys. **33**, 639 (1983); R. Schmitz and E. G. D. Cohen, J. Stat. Phys. **38**, 285 (1985).
- ⁴²B. Kamgar-Parsi and E. G. D. Cohen, Physica **138A**, 249 (1986).
- ⁴³For a recent review, see S. Wolfram, J. Stat. Phys. **45**, 471 (1986).
- ⁴⁴E. G. D. Cohen and I. M. de Schepper, J. Stat. Phys. **46**, 949 (1987).